



New insights from CMS pPb data at $\sqrt{s_{NN}}=8.16$ TeV

SANDRA S. PADULA (FOR THE CMS COLLABORATION)

SPRACE

Intriguing results in pPb collisions at 8.16 TeV

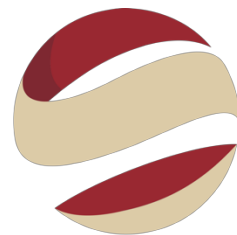
pPb collisions at $\sqrt{s_{NN}} = 8.16$ TeV \rightarrow large data sample (2016):

- 6.4 billion Min Bias events (Multiplicity range: 10 to 185)
- search for jet suppression due to medium interaction (jet quenching)
 - back-to-back jets
 - jet (im)balance \rightarrow ratio of jet $p_T \rightarrow$

$$x_j = \frac{p_T^{j_2}}{p_T^{j_1}}$$

pPb collisions at 8.16 TeV (2016) & PbPb collisions at 5.02 TeV (2018)

- investigate $v_2\{4\}$ at large p_T in pPb and PbPb collisions
 - cumulant method \rightarrow using 0, 2 and 3, 4 subevents (reduces non-flow and back-to-back jets)



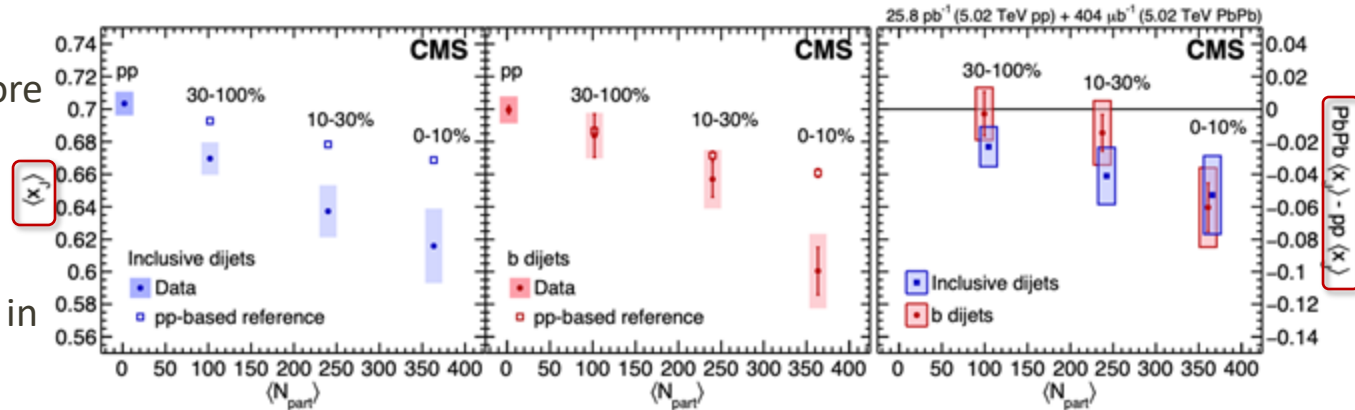
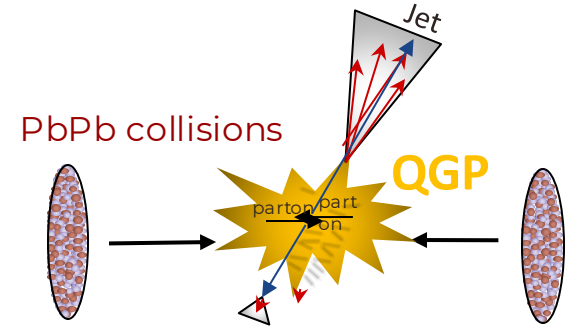
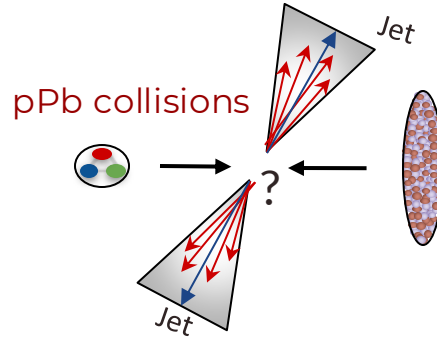
SPRACE

SEARCH FOR JET QUENCHING IN PPB
COLLISIONS AT 8.16 TEV

Jet quenching measured as jet imbalance

Measured in CMS through jet imbalance in PbPb collisions at $\sqrt{s_{NN}} = 5.02$ TeV:

- for inclusive jets
 - quenching increases for more central events (larger multiplicities)
- for b jets
 - clear quenching in 0-10%



$$x_j = \frac{p_{T, \text{Subleading jet}}}{p_{T, \text{Leading jet}}}$$

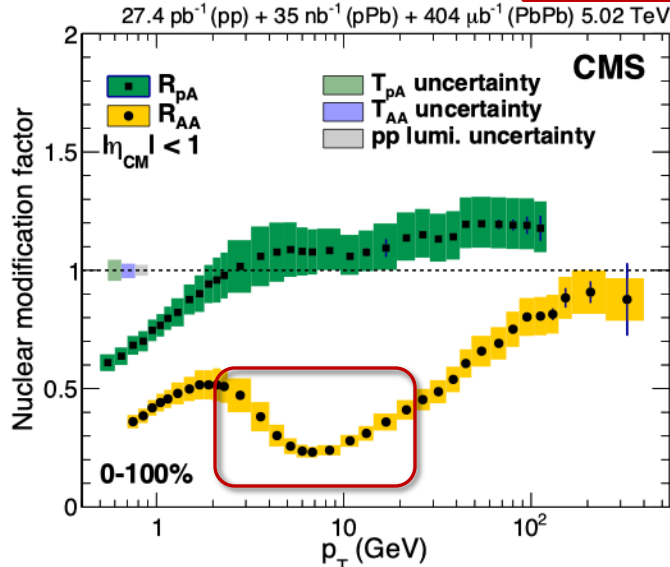
JHEP 03 (2018) 181

CMS R_{AA} and azimuthal anisotropy results

Nuclear modification factors (inclusive centrality class)

- $R_{AA} \rightarrow$ largest suppression in PbPb for $2 < p_T < 30$ GeV
- $R_{pPb} \rightarrow$ no suppression in 2-20 GeV region in **MinBias** pPb

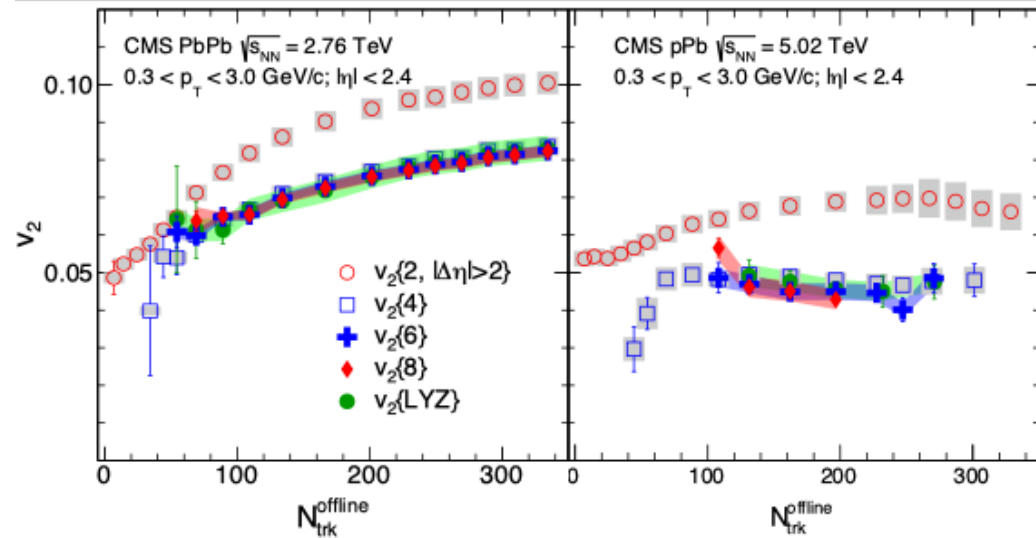
[JHEP 04 \(2017\) 039](#)



Azimuthal anisotropy: low $p_T < 3$ GeV

- observes ridge in pPb
- geometry + fluctuations
- $v_2\{4\} \sim v_2\{6\} \sim v_2\{8\} \rightarrow$ collectivity (High Multiplicity)

[PRL 115, \(2015\) 012301](#)

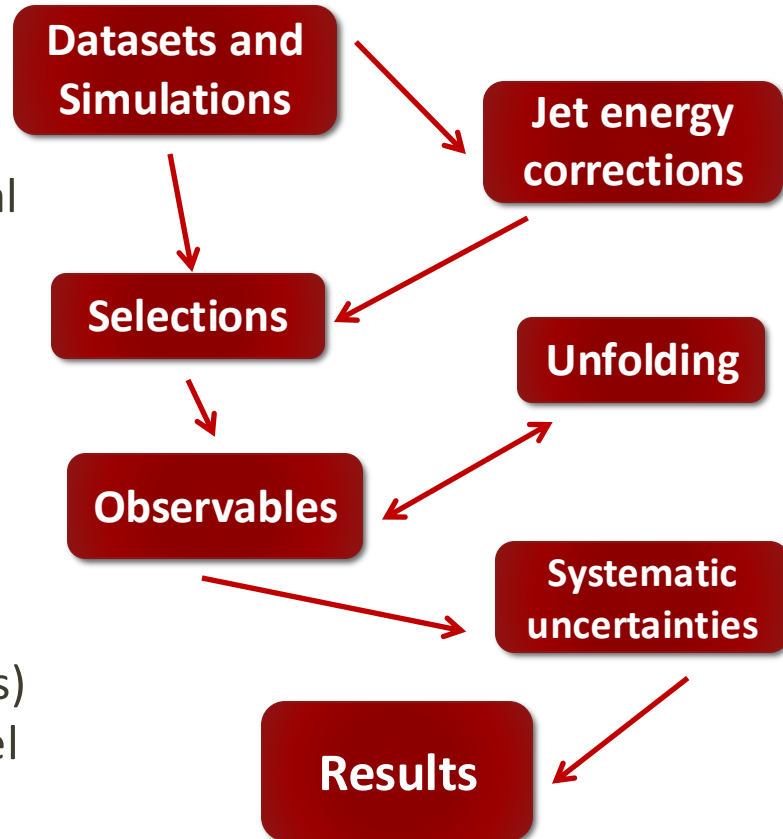


Datasets and MC simulations

pPb@8.16 TeV

- ❑ minimum-bias trigger
 - ~ 6.4 billion Minimum Bias events in total
 - multiplicity range: 10 to 185
- ❑ high multiplicity triggers
 - multiplicity range: 185 to 250
 - ~ 498 Million events in total
 - multiplicity range: > 250
 - ~ 32 Million events in total
- ❑ simulations: PYTHIA8+EPOS
 - ~ 22 million dijet events (all multiplicities)
 - for corrections, unfolding and data-model comparison

Analysis workflow



Measurement setup

Dijet selection

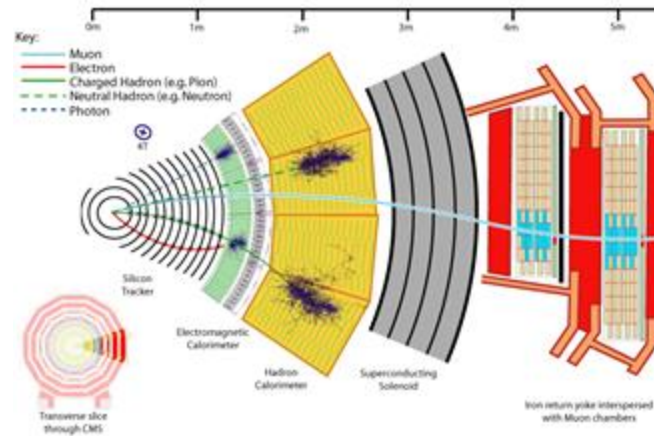
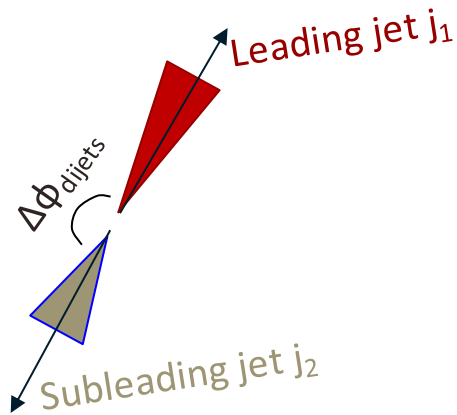
- particle Flow
 - anti- k_T jets with $R = 0.4$
 - $p_T^{j1} > 100 \text{ GeV}$
 - $p_T^{j2} > 50 \text{ GeV}$
 - $|\Delta\phi_{\text{dijets}}| > 5\pi/6$

Observable

$$x_j = \frac{p_T^{j2}}{p_T^{j1}}$$

Analysis methods

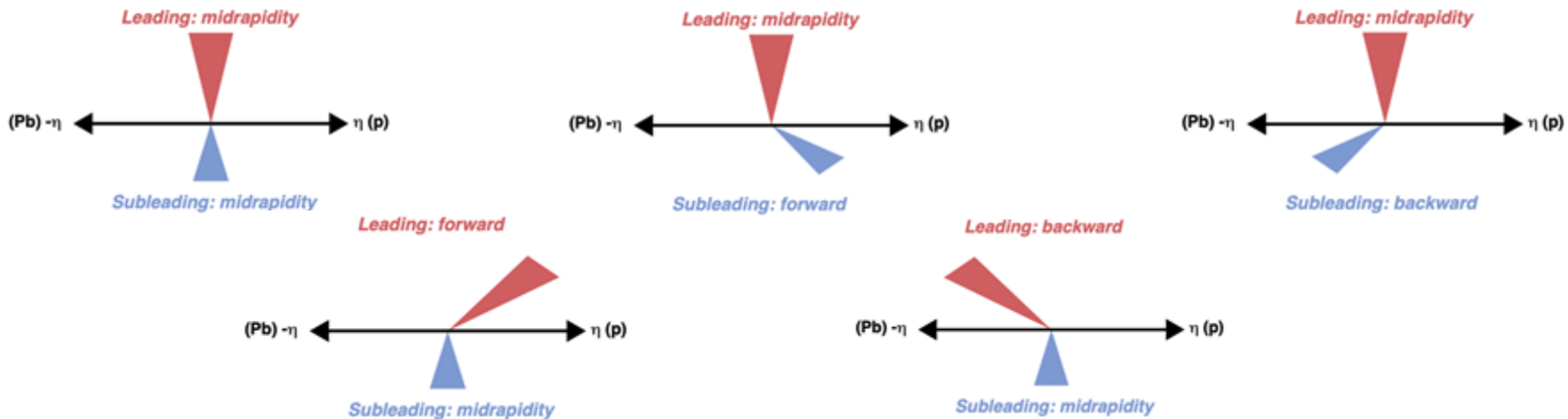
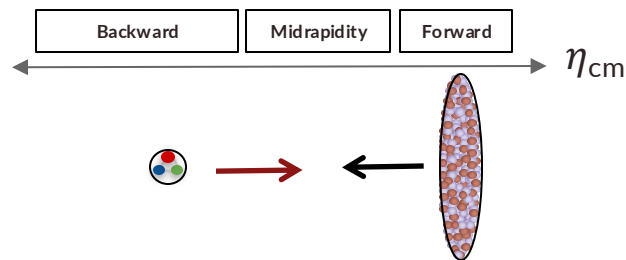
- ratio high-to-low multiplicity (\sim “ R_{CP} -like”)
- probe proton and lead directions (check η dependence)
- apply [D’Agostini unfolding](#) to correct for resolution (first x_j unfolding at CMS)



x_j in different multiplicities and η ranges

Study of x_j as function of multiplicity and pseudorapidity

- ❑ Multiplicity ranges: [10,60], [60,120], [120,185], [185,250] and [250,400]
- ❑ Probe jets in both proton and lead directions
 - Midrapidity: $|\eta_{\text{CM}}| < 1$
 - Forward (p direction): $1.2 < \eta_{\text{CM}} < 2.4$
 - Backward (Pb direction): $-3.3 < \eta_{\text{CM}} < -1.2$
- ❑ Dijet combinations studied:



Unfolding x_j procedure

First x_j unfolding at CMS

- x_j reconstructed vs x_j generated
 - For each η_{CM} combination
 - In different multiplicity bins
 - [10,60], [60,120] and [>120]

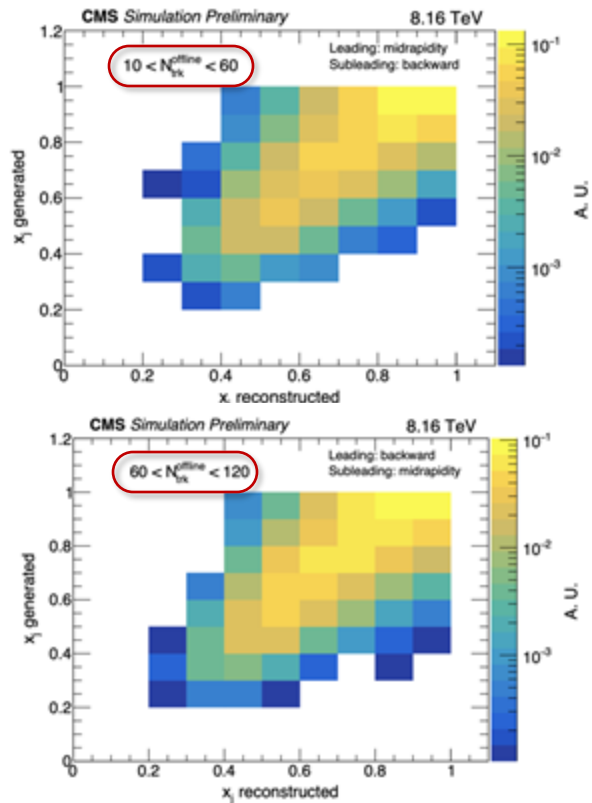
$$x_j = \frac{p_{\text{T}}^{j_2}}{p_{\text{T}}^{j_1}}$$

Effects taken into account in the response matrices

- Fakes \rightarrow Negligible
- Swap $\rightarrow \sim 20\%$
- Missing \rightarrow ROOUnfold
- Data/MC differences
 - $p_{\text{T}}^{j_1}$ vs $p_{\text{T}}^{j_2}$ PDF map applied to the matrices

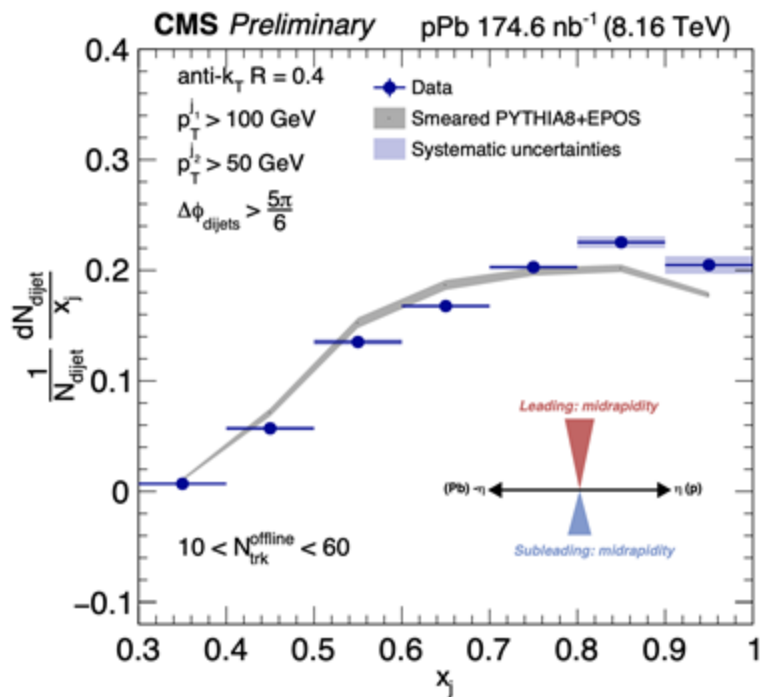
Performed with D'Agostini unfolding via ROOUnfold
Unfolding procedure \rightarrow Validation: MC prior (I) and MC Closure (II) (see backup)

Illustration for 2 $N_{\text{trk}}^{\text{offline}}$ ranges



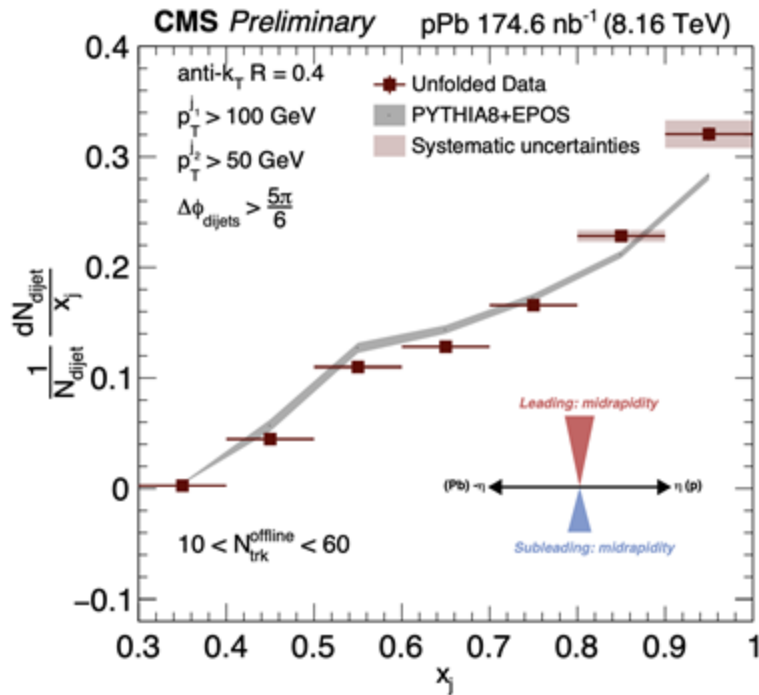
CMS PAS-HIN-23-010

Unfolding x_j – example with data



Smeared results

[CMS PAS-HIN-23-010](#)



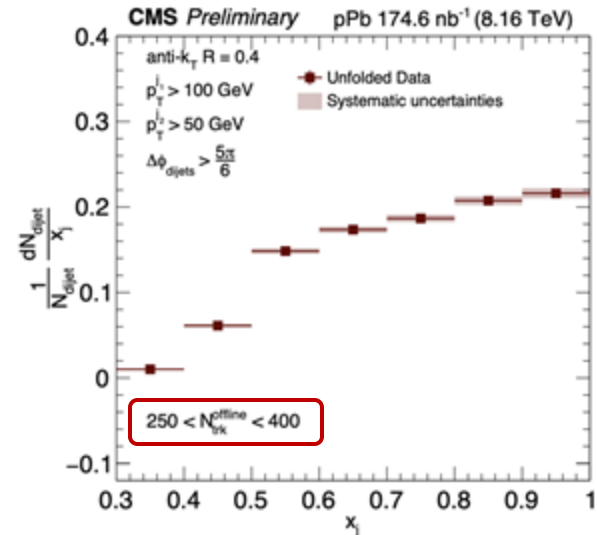
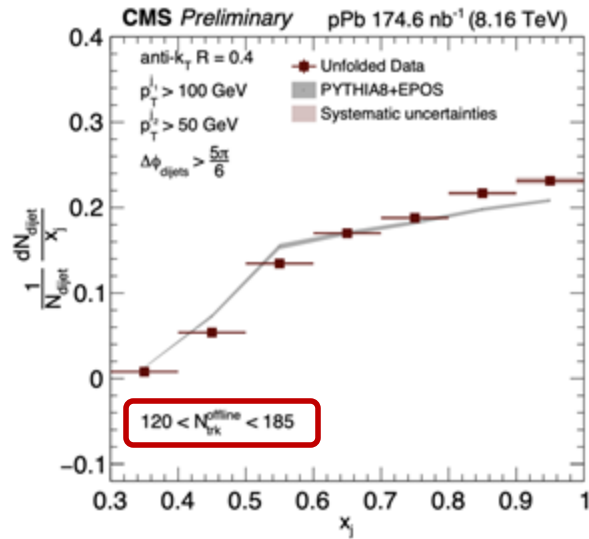
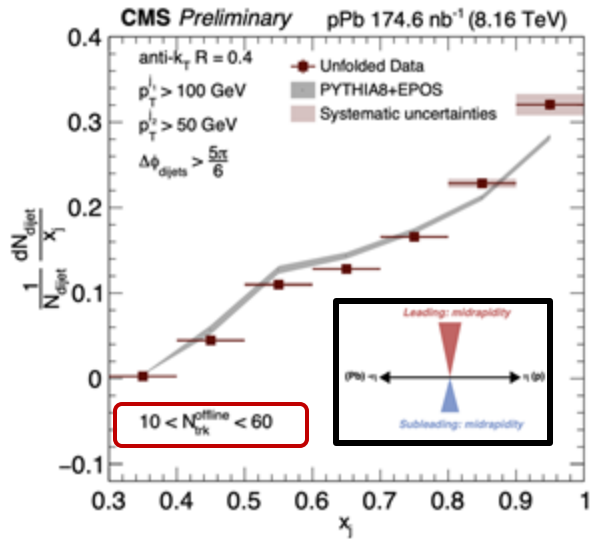
Unfolded results

Results – I: x_j dependence on multiplicity

Changes in shapes seen from low to high multiplicity ranges

- ❑ Especially around $x_j \sim 1$
- ❑ No simulations for the highest multiplicity range

[CMS PAS-HIN-23-010](#)

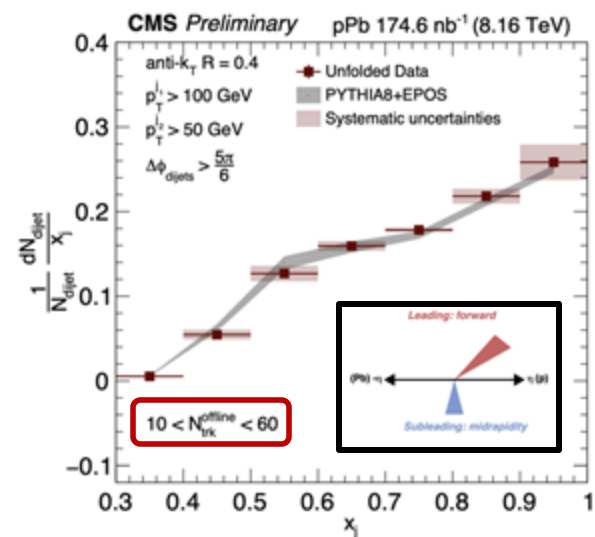
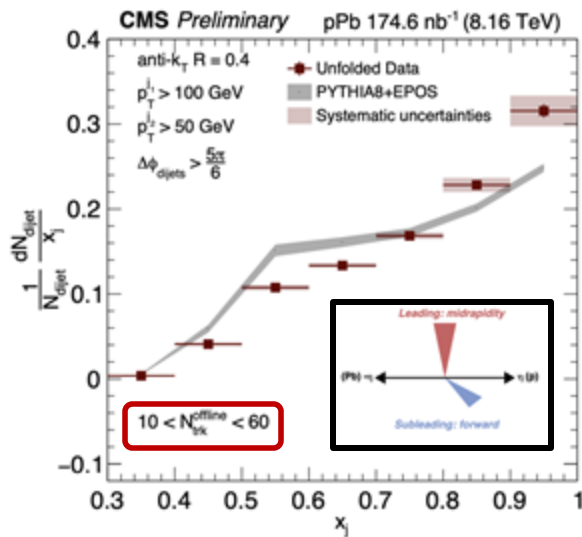
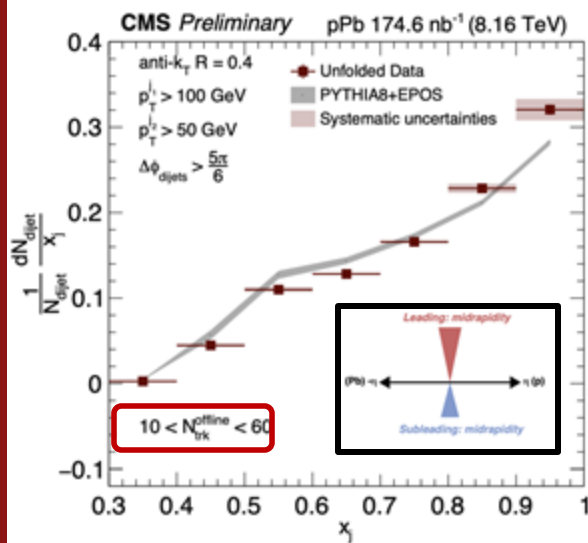


Results – II: x_j dependence on η (forward)

Very similar behavior for all different jet rapidity combinations

- Small changes in shapes
 - results for η backwards are very similar (see backup)

[CMS PAS-HIN-23-010](#)

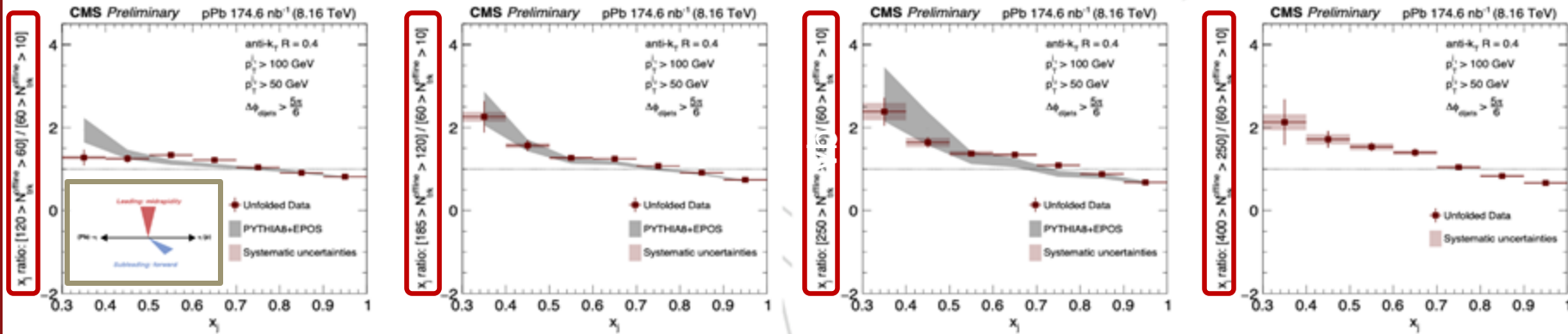


x_j ratios to lowest multiplicity range ($10 < N_{\text{trk}}^{\text{offline}} < 60$)

Useful for cancellation of systematic uncertainties

- Ratio > 1 at low x_j and < 1 for high x_j
- Data well described by PYTHIA8+EPOS MC in all multiplicities and η combinations!
 - PYTHIA8+EPOS do not include energy loss mechanism

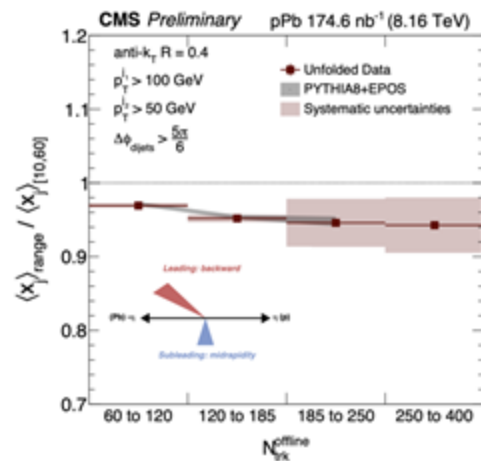
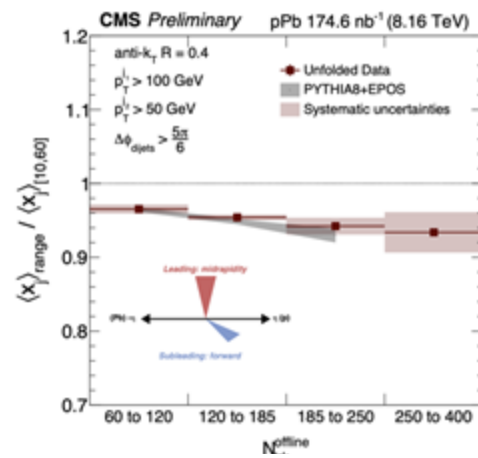
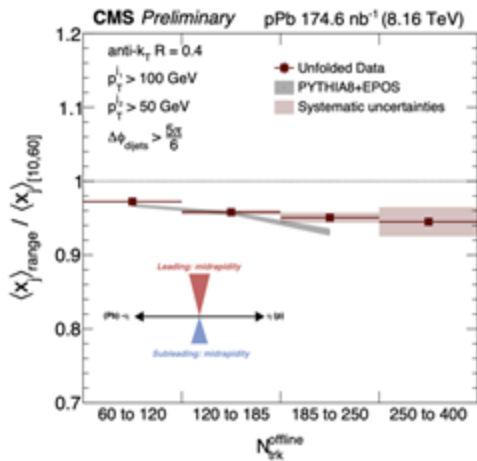
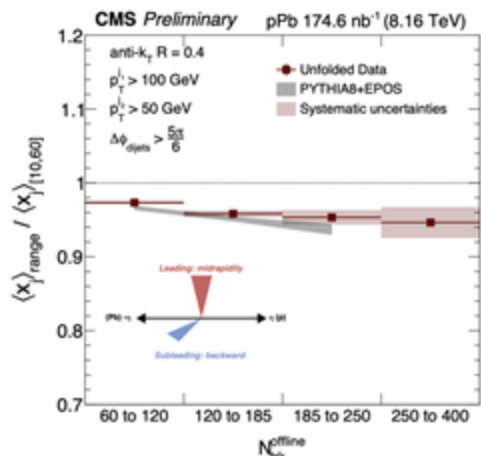
CMS PAS-HIN-23-010



→ Multiplicity

- Possible effects: multijets contribution, energy-momentum conservation, etc.

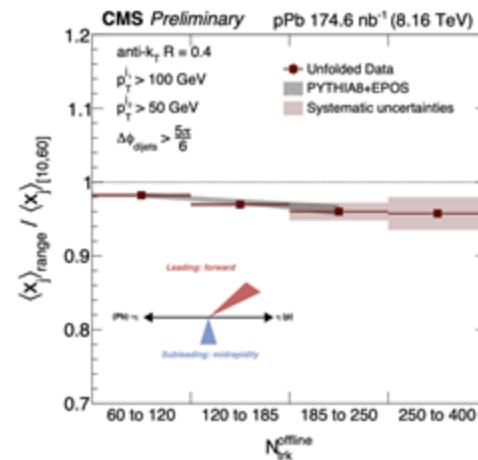
$\langle x_j \rangle$ ratios to lowest multiplicity range ($10 < N_{\text{trk}}^{\text{offline}} < 60$)



Ratio decrease with multiplicity

- Overall good data/MC agreement!
- No clear indication of energy loss!

CMS PAS-HIN-23-010

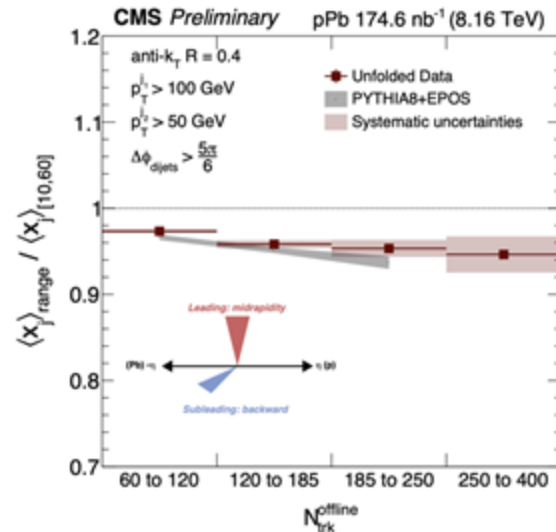
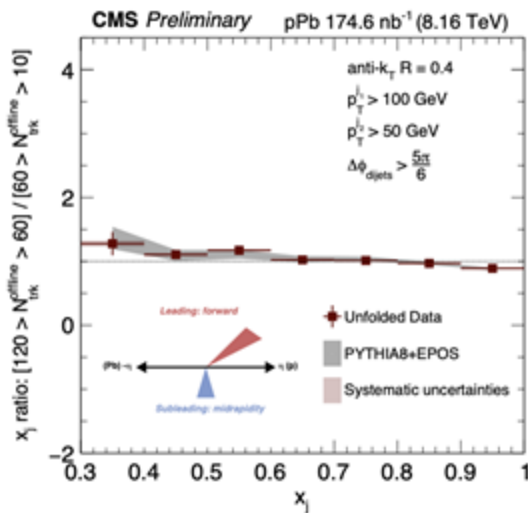
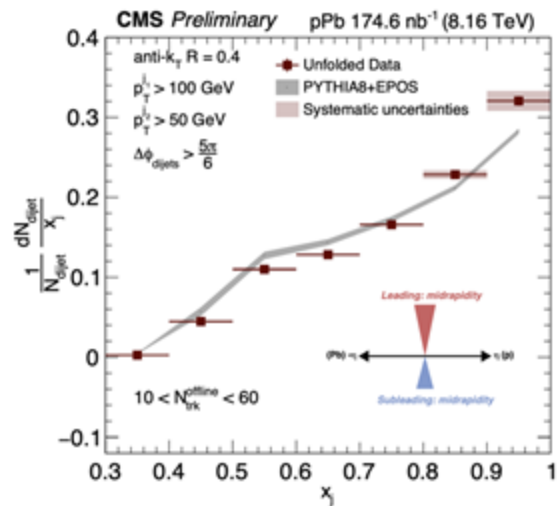


Summary – Part I

First measurement of unfolded x_j using high multiplicity up to $N_{\text{trk}}^{\text{offline}} \sim 400$

- No modifications observed at high multiplicity for any configuration of jet-jet geometry
 - ratio deviations from 1 seen \rightarrow possible effects:
 - Energy-momentum conservation, multijets, among others
 - Well described by PYTHIA8+EPOS (no energy loss)

CMS PAS-HIN-23-010





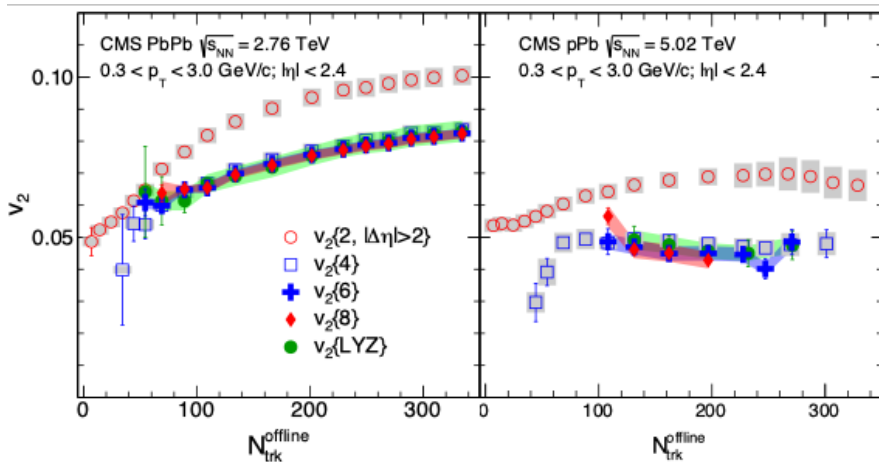
SPRACE

$V_2\{4\} \rightarrow$ CUMULANT METHOD WITH SUBEVENTS

CMS azimuthal anisotropy results at low and at high p_T

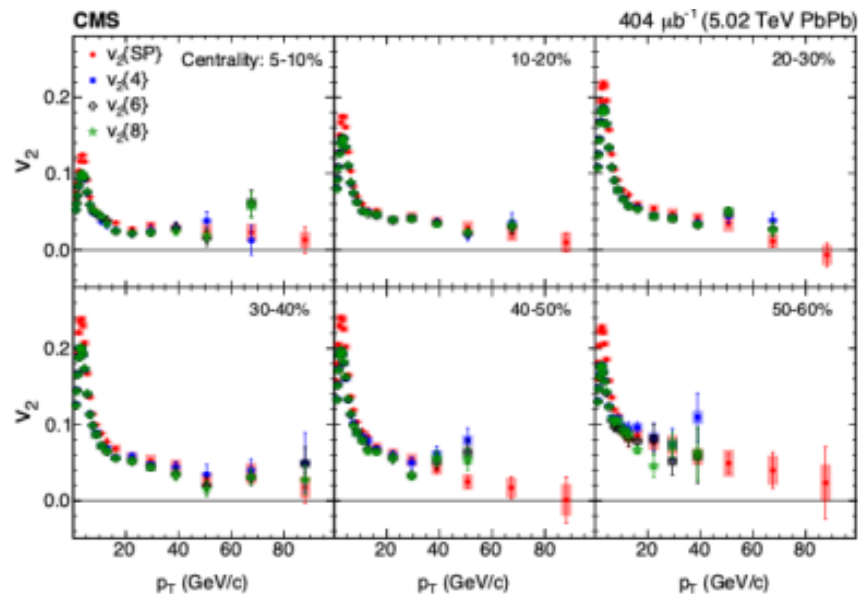
- Azimuthal anisotropy: low $p_T < 3$ GeV
 - observes ridge in pPb
 - geometry + fluctuations
 - well described by hydrodynamics
 - $v_2\{4\} \sim v_2\{6\} \sim v_2\{8\} \rightarrow$ collectivity (High Multiplicity)

[PRL 115, \(2015\) 012301](#)



- Azimuthal anisotropy: high $p_T > 10$ GeV
 - geometry + fluctuations \rightarrow different path lengths of high- p_T parton energy loss in QGP medium
 - v_n at high p_T in PbPb

[PLB 776 \(2017\) 195](#)

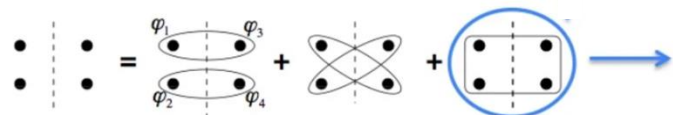


Analysis technique: cumulant method

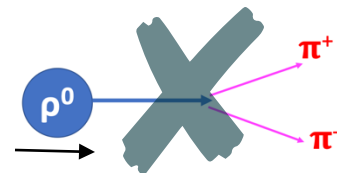
❑ Multiparticle correlation technique

❑ Non-flow suppression

PRC 83 (2011) 044913



$$c_n\{4\} = \langle\langle 4 \rangle\rangle - 2 \cdot \langle\langle 2 \rangle\rangle \langle\langle 2 \rangle\rangle$$



PRC 89 (2014) 064904

Q-cumulant

■ Q-vector: $Q_n \equiv \sum_{i=1}^M e^{in\phi_i}$

$$\langle\langle 2 \rangle\rangle = \langle\langle e^{in(\phi_1 - \phi_2)} \rangle\rangle, \quad \text{and} \quad \langle\langle 4 \rangle\rangle = \langle\langle e^{in(\phi_1 + \phi_2 - \phi_3 - \phi_4)} \rangle\rangle$$

■ cumulants • $c_n\{2\} = \langle\langle 2 \rangle\rangle$ • $c_n\{4\} = \langle\langle 4 \rangle\rangle - 2\langle\langle 2 \rangle\rangle \cdot \langle\langle 2 \rangle\rangle$

■ flow • $v_n\{2\} = \sqrt{c_n\{2\}}$ • $v_n\{4\} = \sqrt[4]{-c_n\{4\}}$

■ differential cumulant :

$$d_n\{4\} = \langle\langle 4' \rangle\rangle - 2 \langle\langle 2' \rangle\rangle \cdot \langle\langle 2 \rangle\rangle$$

1 POI 3 RFPs



(final observable)

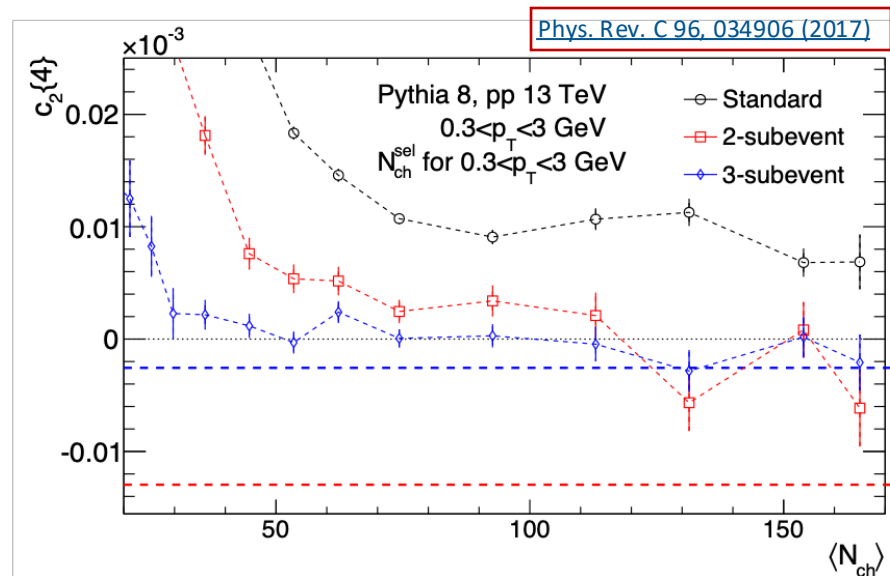
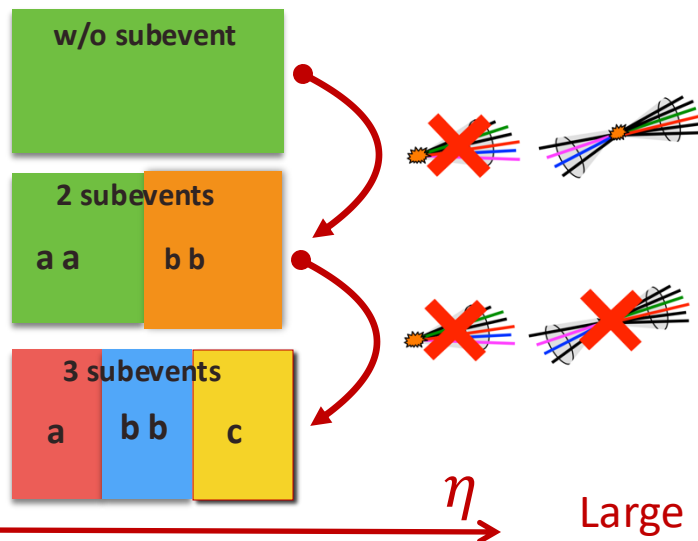
differential flow:

$$v'_n\{4\} = -\frac{d_n\{4\}}{(-c_n\{4\})^{3/4}}$$

Analysis Method

Subevent cumulant techniques

- suppress few-particle correlations for exploring collective correlation signals
- uses subevent cumulant techniques \rightarrow rapidity gaps among the particles
 - 2 subevents \rightarrow can reduce non-flow contribution within the Jets
 - 3 & 4 subevents \rightarrow can remove back-to-back contributions

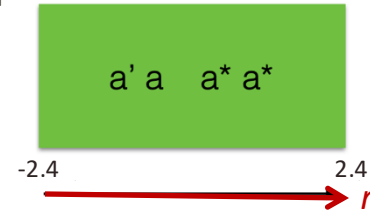


Large η coverage of CMS: enough statistics

Analysis method – I

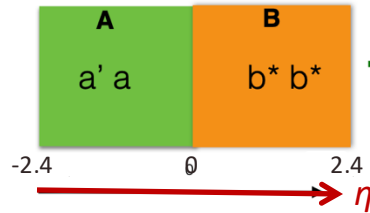
Differential cumulant $d_2\{4\}$: standard and 2 subevent methods

□ standard (no subevents) method

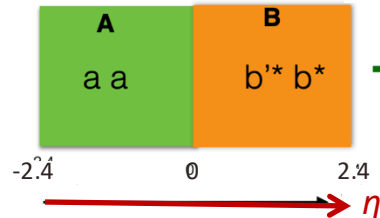


$$d_n\{4\} = \langle\langle 4' \rangle\rangle - 2\langle\langle 2' \rangle\rangle \cdot \langle\langle 2 \rangle\rangle$$

□ 2-subevent method



$$d_n\{4\}_{2sub} = \langle\langle 4 \rangle\rangle^{a' a b b} - 2\langle\langle 2 \rangle\rangle^{a' b} \cdot \langle\langle 2 \rangle\rangle^{a b}$$

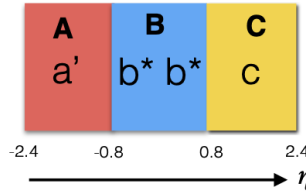


$$d_n\{4\}_{2sub} = \langle\langle 4 \rangle\rangle^{a a b' b} - 2\langle\langle 2 \rangle\rangle^{a b'} \cdot \langle\langle 2 \rangle\rangle^{a b}$$

Analysis method – II

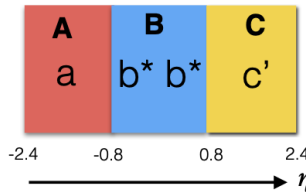
Differential cumulant $d_2\{4\}$: 3 and 4 subevent methods

3-subevent method



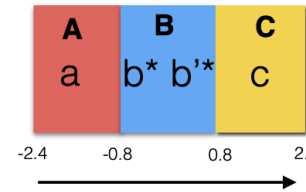
POI : $(-2.4 < \eta < 0.8)$

$$\bullet d_n\{4\}_{3sub} = \langle\langle 4 \rangle^{a' b b^* c}\rangle - 2\langle\langle 2 \rangle^{a' b}\rangle \cdot \langle\langle 2 \rangle^{b^* c}\rangle$$



POI : $(0.8 < \eta < 2.4)$

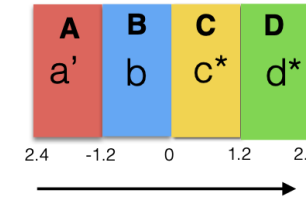
$$\bullet d_n\{4\}_{3sub} = \langle\langle 4 \rangle^{a b b^* c'}\rangle - 2\langle\langle 2 \rangle^{a b}\rangle \cdot \langle\langle 2 \rangle^{b^* c'}\rangle$$



POI : $(-0.8 < \eta < 0.8)$

$$\bullet d_n\{4\}_{3sub} = \langle\langle 4 \rangle^{a b b'^* c}\rangle - \langle\langle 2 \rangle^{a b'}\rangle \cdot \langle\langle 2 \rangle^{b^* c}\rangle - \langle\langle 2 \rangle^{a b}\rangle \cdot \langle\langle 2 \rangle^{b'^* c}\rangle$$

4-subevent method

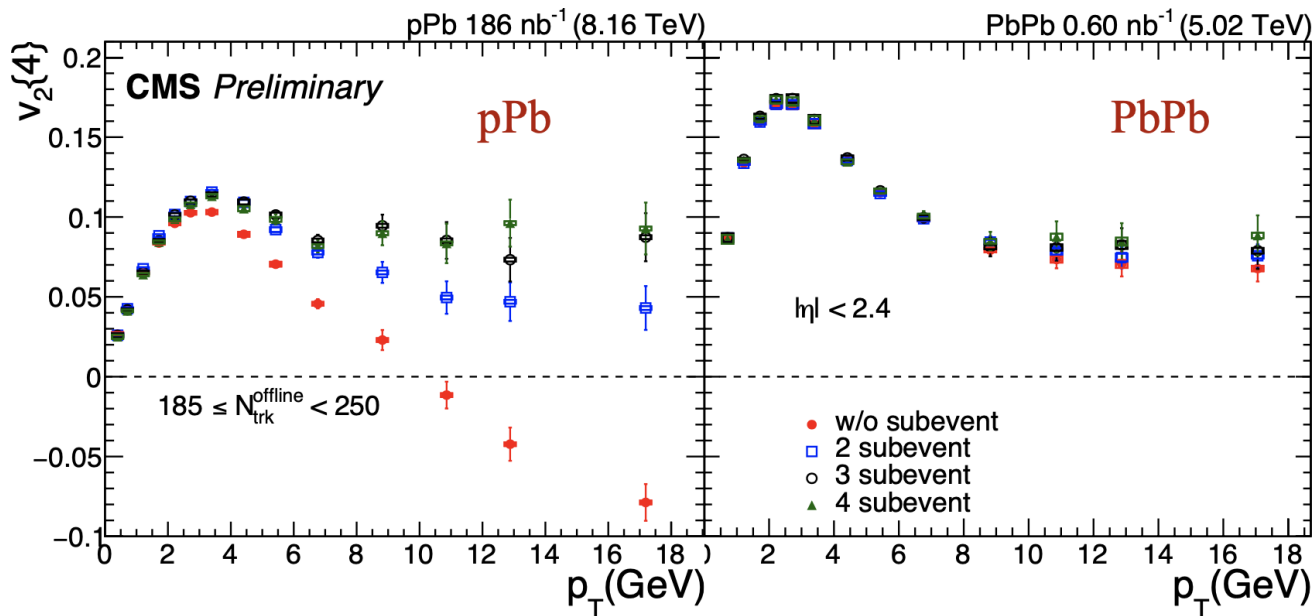


$$d_n\{4\}_{4sub} = \langle\langle 4 \rangle^{a' b c^* d^*}\rangle - \langle\langle 2 \rangle^{a' c^*}\rangle \cdot \langle\langle 2 \rangle^{b d^*}\rangle - \langle\langle 2 \rangle^{a' d^*}\rangle \cdot \langle\langle 2 \rangle^{b c^*}\rangle$$

Results

$v_2\{4\}$ in $185 \leq N_{\text{trk}}^{\text{offline}} < 250$ as a function of p_T

CMS-PAS-HIN-23-002



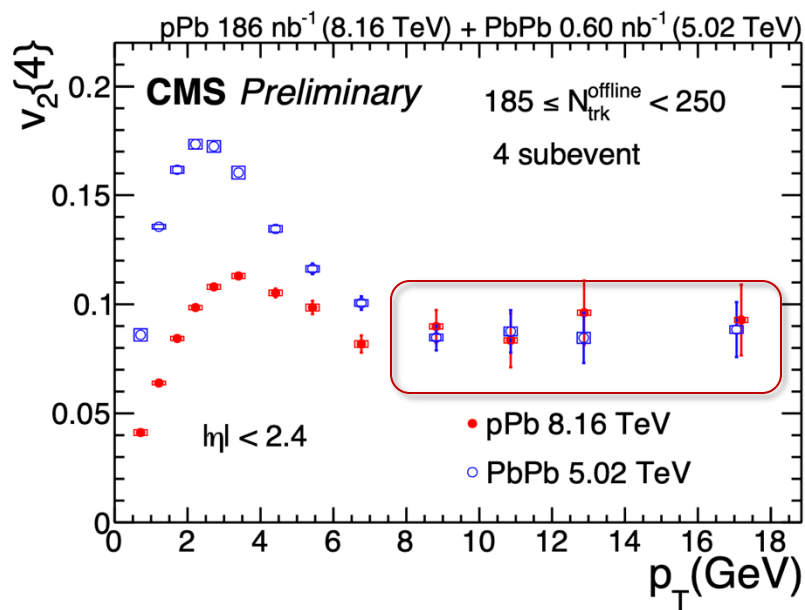
At low p_T : PbPb has larger $v_2\{4\}$ than pPb

At high p_T : similar magnitude and similar trend of subevents $v_2\{4\}$

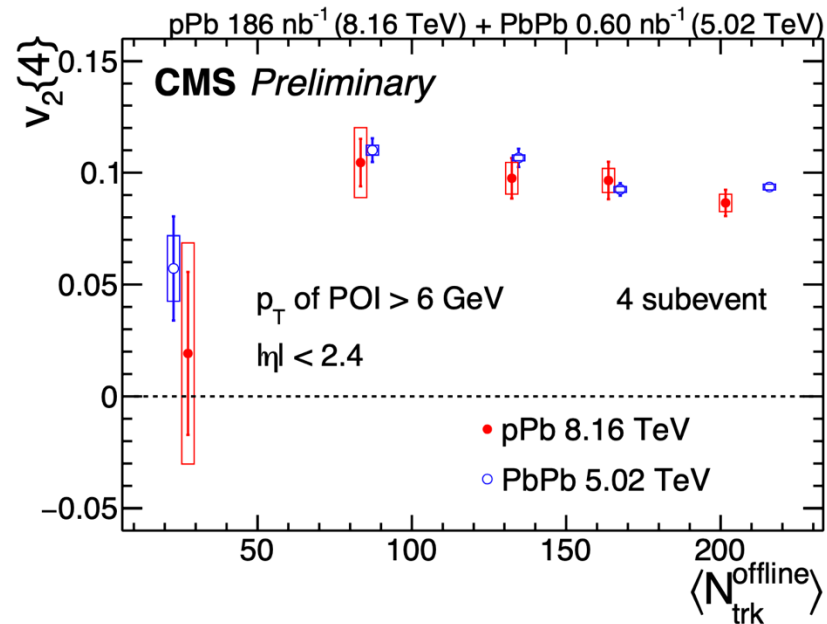
Results: 4-subevent $v_2\{4\}$...

CMS-PAS-HIN-23-002

... for $185 \leq N_{\text{trk}}^{\text{offline}} < 250$ versus p_T



... for $p_T^{\text{POI}} > 6$ GeV versus $\langle N_{\text{trk}}^{\text{offline}} \rangle$

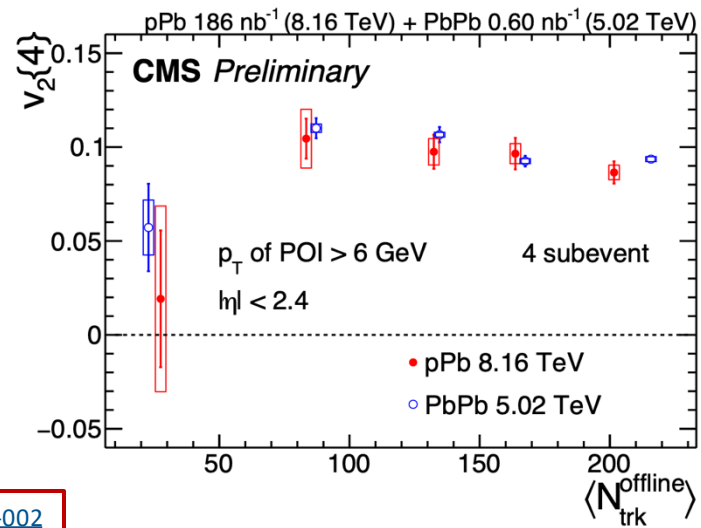
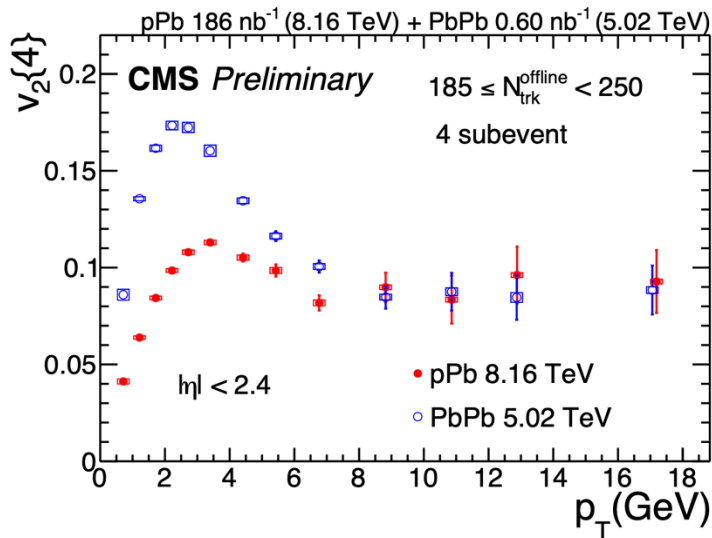


Summary – part II

$v_2\{4\}$: subevents for pPb at $\sqrt{s_{NN}} = 8.16$ TeV & PbPb collisions $\sqrt{s_{NN}} = 5.02$ TeV

- Extended phase space investigated for the first time in small systems
 - insights into potential indication of high- p_T parton energy loss
- significant positive value for $v_2\{4\}$ at high p_T in pPb collisions after removing nonflow with subevent methods
- striking similarity of high multiplicity pPb and peripheral PbPb collisions \rightarrow similar mechanism?

These results provide new information on the interaction of high- p_T partons with the medium in collisions of small system





Thank you!!

This material is based upon work supported by the São Paulo Research Foundation (FAPESP) Grants No. 2018/01398-1 and No. 2013/01907-0. Any opinions, findings, and conclusions or recommendations expressed in this material are those of the author(s) and do not necessarily reflect the views of FAPESP

BACK UP SLIDES

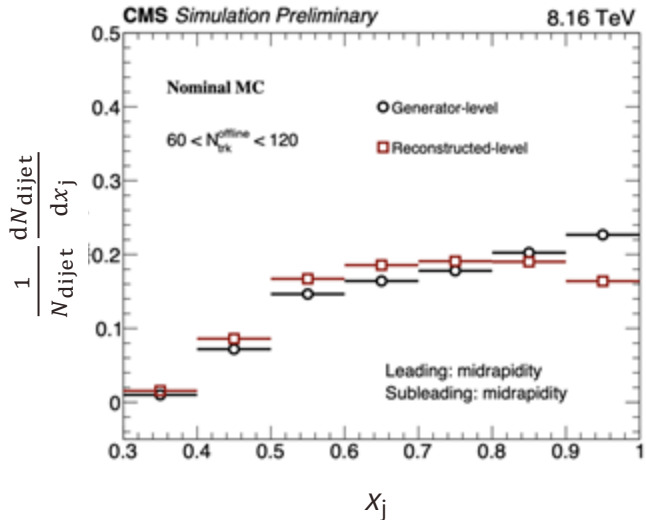
Validate the unfolding procedure at MC (I): prior

Data/MC reconstructed pdf (p_{T}^{j1}, p_{T}^{j2}) \rightarrow applied to remove sensitivity to prior shape

Procedure is tested using an “oversampled MC”

- Very different prior between the nominal and oversampled test-MC

Nominal MC
(PYTHIA+EPOS)

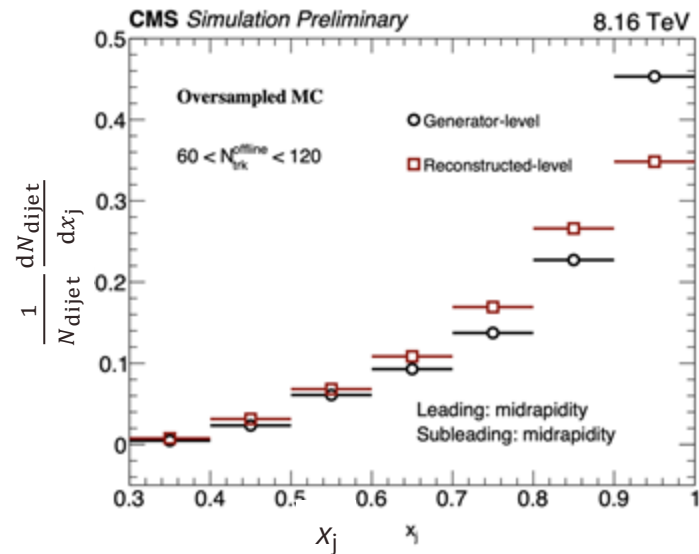


(very different distributions!)

[CMS PAS-HIN-23-010](#)

Oversampled MC

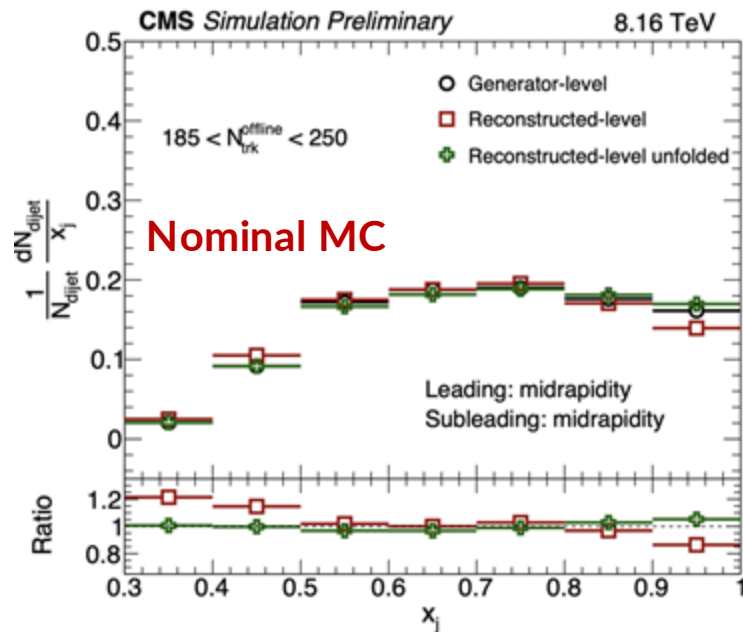
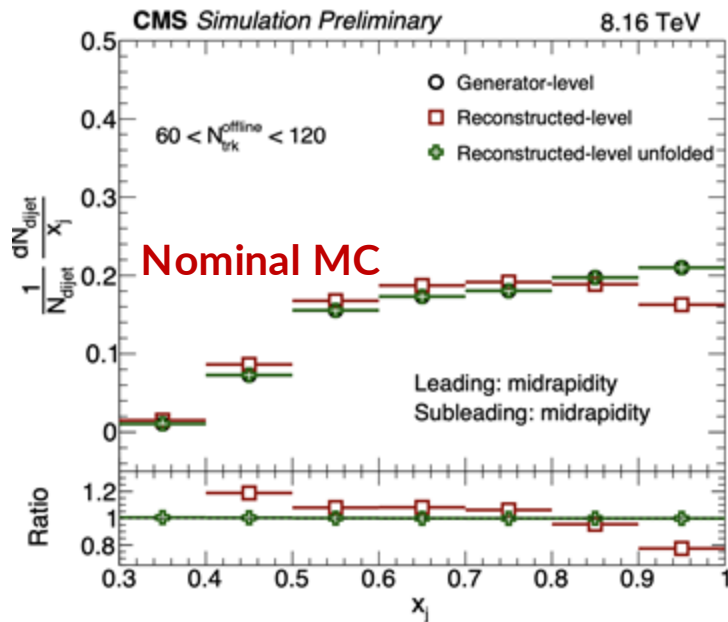
(PYTHIA+EPOS, no invariant p_T rescale)



Validate the unfolding procedure at MC (II): closures

Closures achieved even with drastically different priors!

- Shows advantage of using the pdf-convoluted response matrices for cases when no reliable Monte Carlo exists



CMS PAS-HIN-23-010

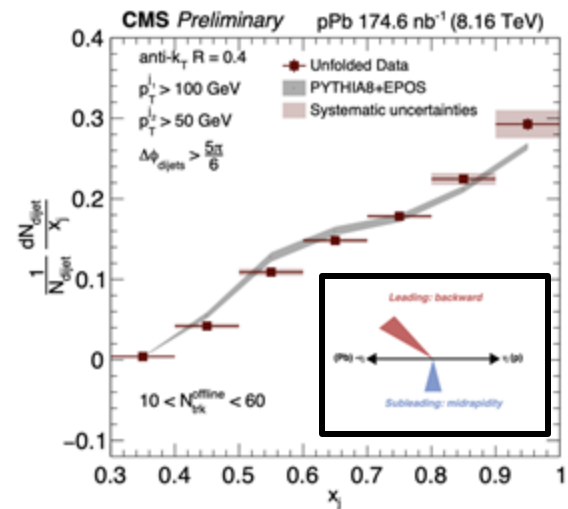
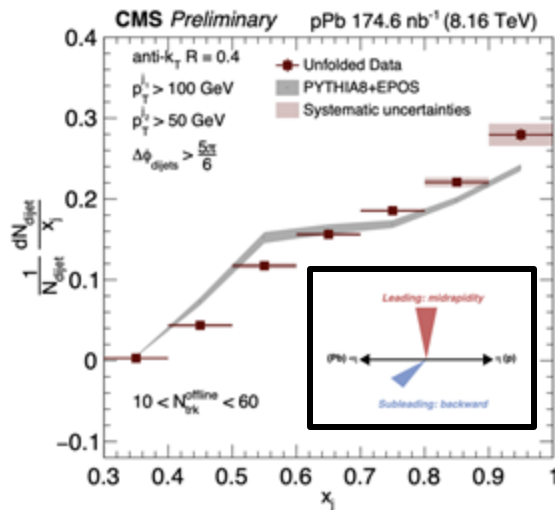
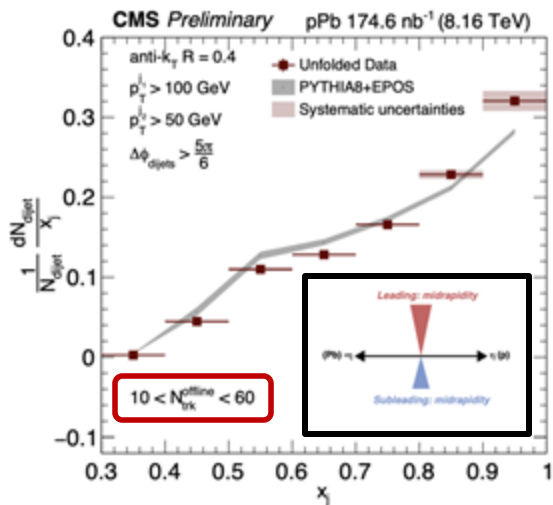
Results – III: x_j dependence on η (backward)

Very similar behavior for all different jet combinations

□ Small changes in shapes

■ results for η backwards are very similar (see backup)

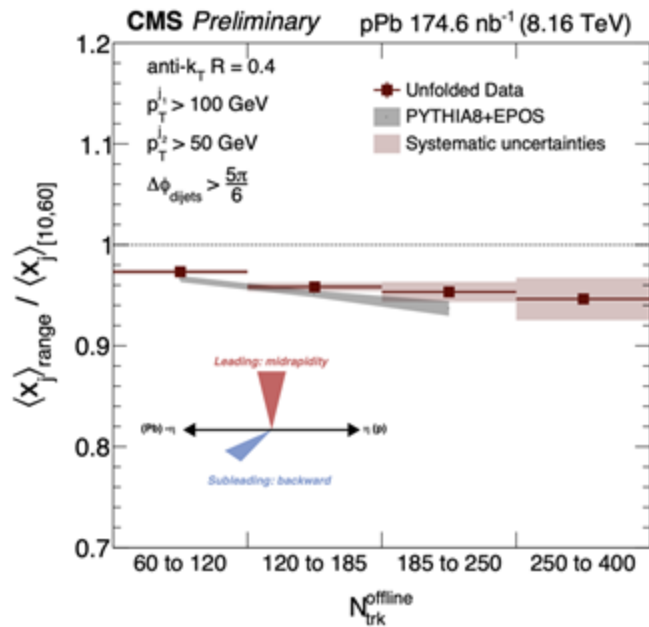
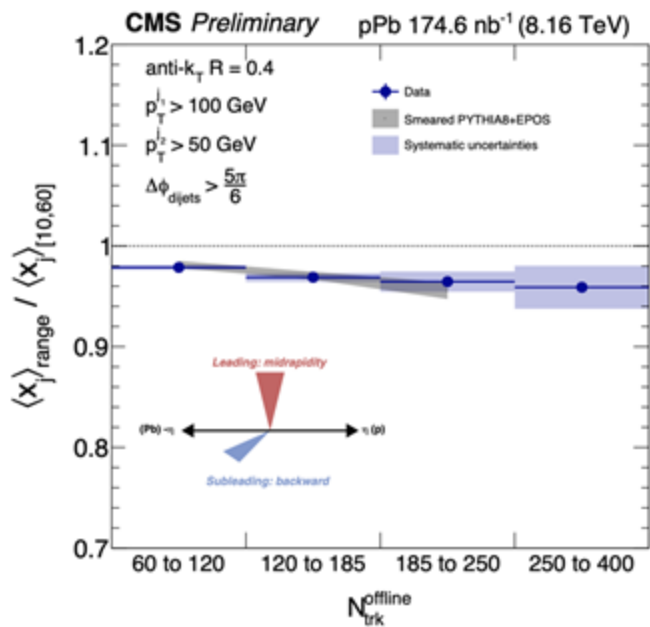
[CMS PAS-HIN-23-010](#)



$\langle x_j \rangle$ ratio high-to-low multiplicities: reco vs. unfolded

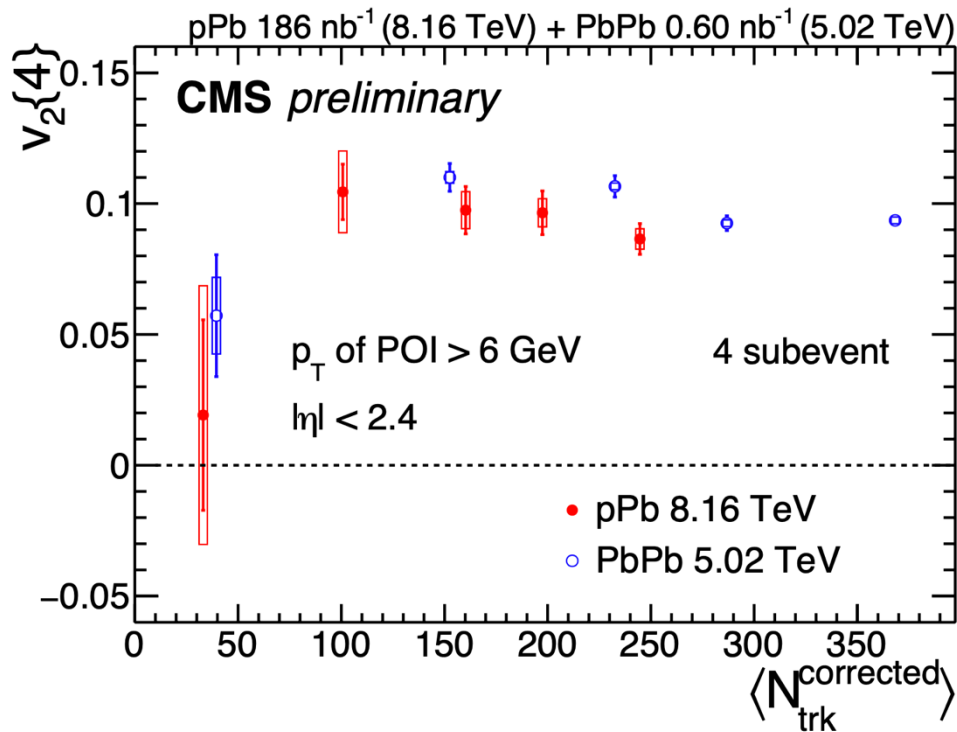
- ❑ Similar behavior between reconstructed and unfolded
- ❑ Ratio decrease with multiplicity
- ❑ Overall good data/mc agreement

[CMS PAS-HIN-23-010](#)



Supplement: $v_2\{4\}$ cumulant with subevents

$v_2\{4\}$ in different $\langle N_{trk}^{corrected} \rangle$ bins with POI $p_T > 6$ GeV

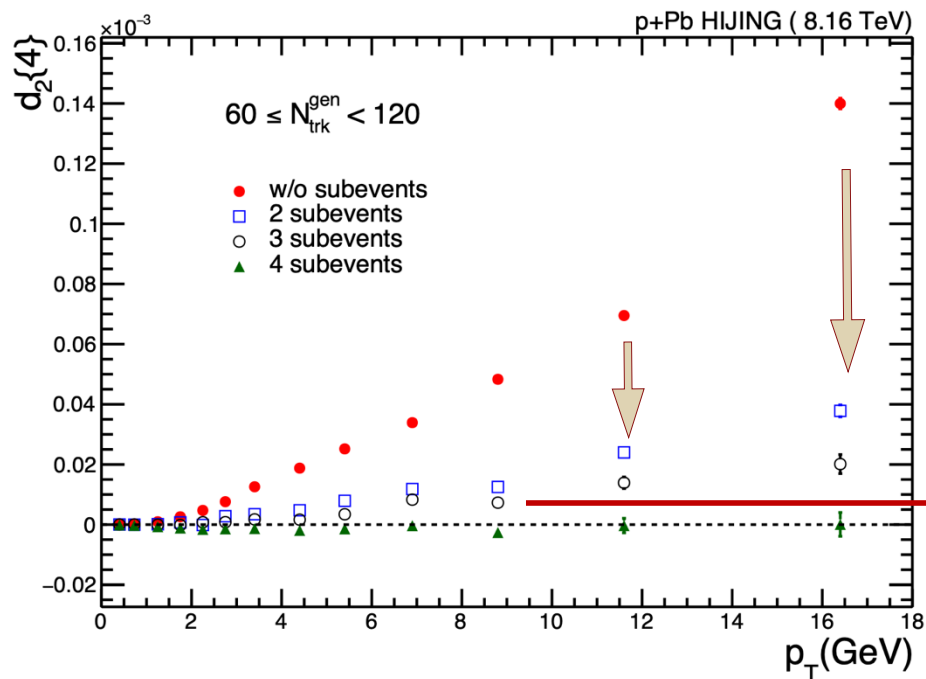


$N_{trk}^{offline}$ range	pPb		PbPb	
	$\langle N_{trk}^{offline} \rangle$	$\langle N_{trk}^{corrected} \rangle$	$\langle N_{trk}^{offline} \rangle$	$\langle N_{trk}^{corrected} \rangle$
(0, 60)	27	33±1	23	39±2
[60, 120)	83	101±4	87	152±6
[120, 150)	132	160±6	135	233±10
[150, 185)	164	198±7	168	287±12
[185, 250)	202	245±10	216	368±16

CMS-PAS-HIN-23-002

Cross-check with simulation

$d_2\{4\}$ in HIJING in $60 \leq (N_{trk}^{gen}) < 120$



$d_2\{4\}$ in data

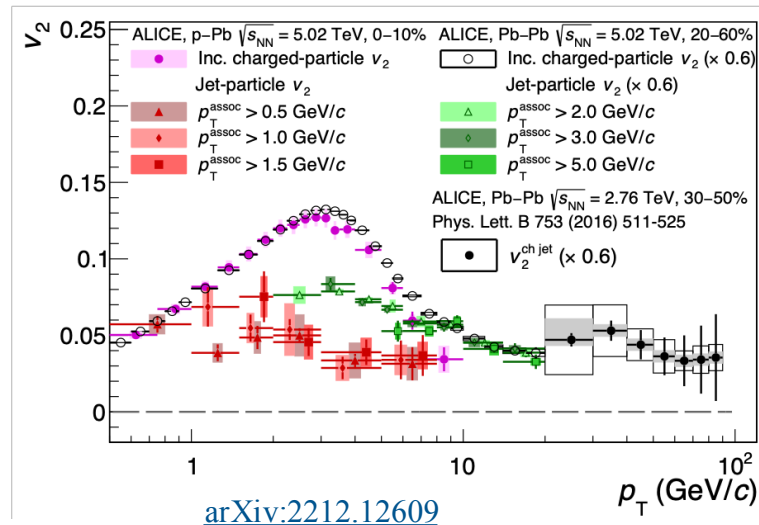
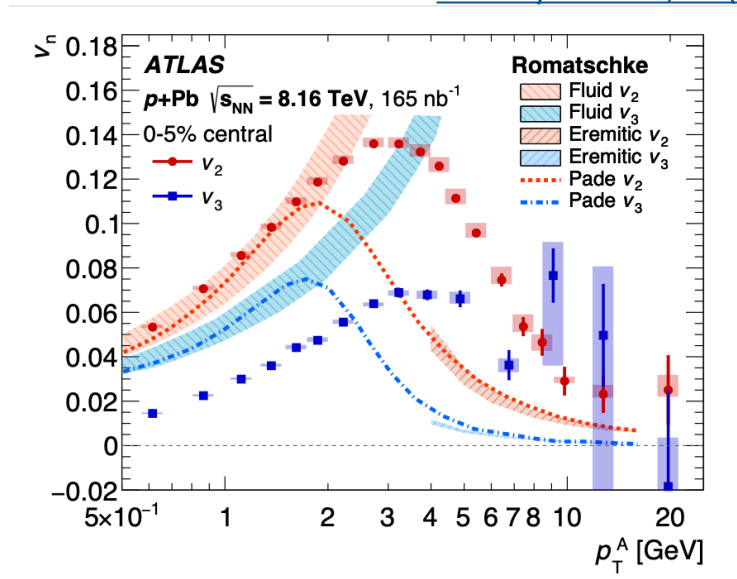
HIJING

□ no collectivity

□ employed to cross check non-flow subtraction of subevent cumulant

Previous Measurements of v_n in pPb at High p_T

[Eur. Phys. J. C 80, 73 \(2020\)](#)



- 2-particle correlation technique (nonflow contamination)
- Template fit method for nonflow subtraction
- Based on strong assumptions